

Effects of Composition and Temperature on Site Occupancies and Antisite Defects in B2-FeAl Ordered Phase: A Phase Field Study

Wang Kun¹, Wang Yongxin¹, Hu Shi², Chen Zheng¹, Cheng Yanfeng¹

¹ State Key Laboratory of Solidification Processing, Northwestern Polytechnical University, Xi'an 710072, China; ² Civil Aviation Flight University of China, Guanghan 618307, China

Abstract: The site occupancies and antisite defects play an important role in the physical and mechanical properties of intermetallic compound alloys. In this paper, the effects of Al concentration (c_{Al}) and temperature (T) on the change trend of site occupancies and antisite defects in B2-FeAl, which has attractive properties, were investigated by phase field method. The numerical results show that the increase of c_{Al} or the decrease of T can result in an acceleration of solute atoms segregation in matrix phase, and make site occupancies of Al and Fe as well as antisite Fe/Al reach equilibrium state earlier. Meanwhile, the increase of c_{Al} or the decrease of T can enhance the site occupancies of Fe and Al and reduce the two types of antisite defects. Furthermore, the theoretical results show that the change of c_{Al} and T is not able to change the main type of antisite defect in B2-FeAl ordered phase.

Key words: B2-FeAl; site occupancy; antisite defect; temperature and composition; phase field

Because the B2-FeAl intermetallic compound has excellent characteristics of moderate/high temperature properties, strength-to-weight ratio, corrosion and oxidation resistance^[1], it becomes a competitive material among high temperature intermetallic compounds. In addition, compared with other compounds, its cheap raw material costs and abundance reserves make it have some advantages in manufacturing.

Previously, study of B2-FeAl is mainly experimental research, such as the effect of thermal vacancy on high temperature yield-stress anomaly^[2], the influence of Al concentration on Fe-vacancy^[3, 4], the impact of B doping on the mechanical manifestation^[5]. Some work is also conducted from the theoretical perspective, for example, selecting doping elements for improvement of B2-FeAl brittleness through First-principles calculation^[1], effect of growing antiphase domains on restoring the long range order of FeAl^[6], the impact of the first nearest-neighbor interaction energy on vacancy concentration^[7].

In the recent years, attention of materials scientists is paid on the site occupancies and antisite defects in intermetallic compounds^[8-11]. Knowledge of the site occupancies and antisite defects in B2-FeAl is of great importance since they can influence the bonding characteristics and consequently change the material properties. In order to understand the properties of B2-FeAl and develop it to a practical engineering material, investigation on the site occupancies and antisite defects formed in B2-FeAl ordered phase is very necessary. However, the effects of alloy composition and temperature on site occupancies and antisite defects in B2-FeAl are seldom touched. In this work, the phase field method based on master kinetic equation is employed to determine the effects of Al concentration and temperature on the site occupancies and antisite defects in B2-FeAl order phase.

1 Master Kinetic Equation for the Simulation

The kinetic equation was brought forward by

Received date: July 25, 2018

Foundation item: National Natural Science Foundation of China (51475378, 51575452, 51474176, 51704243)

Corresponding author: Wang Yongxin, Ph. D., Professor, State Key Laboratory of Solidification Processing, Northwestern Polytechnical University, Xi'an 710072, P. R. China, E-mail: wyx818@126.com

Copyright © 2019, Northwest Institute for Nonferrous Metal Research. Published by Science Press. All rights reserved.

Khachatryan^[12]. In this equation, the micro-alloying process is described by a time-dependent changing frequency which is called arbitrary atomic occupation probability of single site (AOPSS) at perfect crystal lattice. The AOPSS is a discrete function, which is described as:

$$\frac{d\phi(r, t)}{dt} = \frac{(c - c^2)}{k_B T} \sum_{r'} L_0(r, r') \frac{\partial F}{\partial \phi(r', t)} \quad (1)$$

Where, c is the average solute Al concentration, k_B denotes Boltzmann constant, T is the absolute temperature and F is the total free energy. $L_0(r, r')$ is the coefficient matrix related with Fe-Al atom inter-diffusion. It has been proved that this model is capable of modeling phase transition^[13,14] and tracing single atom diffusion^[15]. More details of this model can be found in Refs. [16-20].

The Fourier transformation is used to solve Eq.(1), and the solving result is written as:

$$\frac{d\phi(\mathbf{k}, t)}{dt} = \frac{(c - c^2)}{k_B T} \sum_r L_0(\mathbf{k}) [V(\mathbf{k})\phi(\mathbf{k}, t) + k_B T \ln \frac{\phi(\mathbf{k}, t)}{1 - \phi(\mathbf{k}, t)}] + \zeta(\mathbf{k}) \quad (2)$$

In Eq.(2), \mathbf{k} denotes the reciprocal lattice vector corresponding to body-centered cubic Fe-Al alloys^[19]. And $\mathbf{k} = 2\pi(h\mathbf{a} + k\mathbf{b} + l\mathbf{c})$, where a, b, c are unit reciprocal lattice vectors of Fe-Al lattice along [100], [010] and [001] directions, respectively^[14,19]. $\zeta(\mathbf{k})$ is the noise term following the fluctuation dissipation theory^[17,18]. The straightforward Fourier results of Fe-Al interchange energy $V(\mathbf{k})$ and coefficient matrix $L_0(\mathbf{k})$ are expressed as^[17]:

$$V(\mathbf{k}) = 8v_1 \cdot \cos \pi h \cdot \cos \pi k \cdot \cos \pi l + 2v_2 [\cos 2\pi h \cdot \cos 2\pi k \cdot \cos 2\pi l] + \dots \quad (3)$$

$$L_0(\mathbf{k}) = 8L(\cos \pi h \cdot \cos \pi k \cdot \cos \pi l - 1) \quad (4)$$

Where, (h, k, l) is the coordinate of \mathbf{k} . v_i ($i=1, 2, 3, \dots$) are the Fe-Al ordering energies for the first, second, third, ..., coordination spheres. In plane coordinate, Eqs.(3) and (4) cannot involve all Fe- and Al- sublattices in the Cartesian coordinate. Therefore, the primitive cell is re-defined for the {001} planes. The use of the new primitive cell can accurately reflect any lattice site in the {001} plane. Combined with the Cartesian coordinate transformation, the new Fourier transformation of $V(\mathbf{k})$ and $L_0(\mathbf{k})$ can be changed into the following forms:

$$V(\mathbf{k}) = 8v_1 \cdot \cos \pi(h+k) \cdot \cos \pi(h-k) + 2v_2 [\cos 2\pi(h+k) \cdot \cos 2\pi(h-k)] + 2v_2 + \dots \quad (5)$$

$$L_0(\mathbf{k}) = 8L[\cos \pi(h+k) \cdot \cos \pi(h-k) \cdot \cos \pi l - 1] \quad (6)$$

Where, the constant L is equal to $1^{[12]}$.

The first and second nearest ordering energies of Fe-Al ($v_1=12 \times 10^{-7}$ J, $v_2=6.8 \times 10^{-7}$ J^[21,22]) are capable of describing B2 FeAl structure during the solid-state transformation. Using the

transformed $V(\mathbf{k})$ and $L_0(\mathbf{k})$, a phase field model for the A2 to B2 solid transformation is established.

2 Results and Discussion

In this work, the simulation was performed in a square space scaled by 104 nm×104 nm. According to the experiment^[3, 23] and theory^[22] studies, Al concentrations $c_{Al}=0.29, 0.31, 0.33, 0.35, 0.37$ (in unit of atomic fraction) were selected to investigate the effect of Al concentration, and temperatures $T=793, 853, 913, 973$ K were selected to study temperature effect. B2-FeAl phase exists under this parameter selections of T and c_{Al} ^[24,25].

2.1 Morphology of B2-FeAl phase domain and atomic structure of B2

Fig.1 shows the microstructural morphologies of B2-phase domain with different Al concentrations obtained by the phase field method. The phase domains (uniform color parts) are separated by phase domain boundaries (blue curves) in different frames. The magnified picture in each frame shows the atomic structure of B2-FeAl phase domain, in which the mazarine squares represent Fe atoms and other squares denote Al atoms. Microstructures (Fig.1) demonstrate that the nonstoichiometric ordered FeAl phases at different Al contents contains several anti-phase domain boundaries (APDBs) separating finer domains, which is a result of congruent ordering decomposition. Comparing the panels of Fig.2, no evident difference exists for the ordered phases containing nanometer domains. As there is no morphological distinction between nanoscale APDBs in single ordered B2 phase, microstructure maps at different temperatures are not displayed here. The color of each square is associated with AOPSS and this correlation is visually reflected by the colorbar in Fig.1. The relationship between simulated planar B2-cell and actual crystal cell is demonstrated in Fig.1f. Normally, for an ideal ordered B2-FeAl intermetallic compound, the body center site is occupied by Al atom and eight corner sites are occupied by Fe atoms. The site occupancy can be denoted as $Fe_{Fe} (Al_{Al})$ which means that Fe (Al) atom is in Fe-sublattice (Al-sublattice) site. And if Fe (Al) atom is located in Al-sublattice (Fe-sublattice) site, the antisite defect forms, which can be expressed as $Fe_{Al} (Al_{Fe})$. In Fig.1, the effects of c_{Al} on site occupancies and antisite defects are directly reflected by color discrepancy. However, as color discrepancy is not accurate enough, we use the time-dependent variation of AOPSS to reveal the effects of c_{Al} and T on site occupancies and antisite defects in the following sections.

2.2 Effect of Al concentration on site occupancies and antisite defects

To reveal the effect of c_{Al} on site occupancies and antisite defects, the aging processes of systems with different Al concentrations at 853 K were calculated. The temporal site occupancies are displayed through AOPSS

curves as shown in Fig.2.

According to Fig.2, the ordering process undergoes three stages: incubation period, solute atoms segregation period (SASP) and equilibrium period. The flat curves in Fig.2a₁ and

2b₁ describe the distributions of Fe and Al in incubation period and SASP. In the incubation period, the alloy system still sustains the initial disordered state; hence, the AOPSS of Al in each site is equal to the initial c_{Al} . Compared with disordered

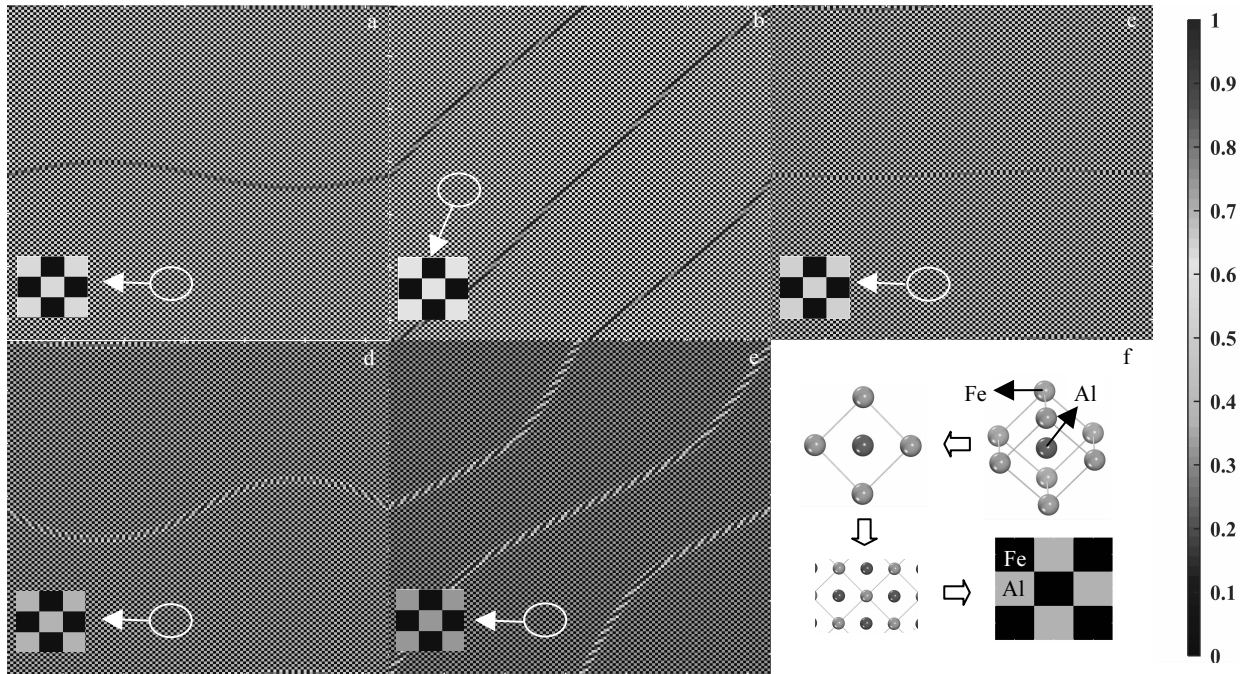


Fig.1 Morphologies of B2-FeAl phase domain at 853 K with different Al concentrations (c_{Al}): (a) 0.29, (b) 0.31, (c) 0.33, (d) 0.35, (e) 0.37, and (f) relationship between simulated planar B2-cell and actual crystal cell (the web version of this paper provides a better comprehension of this figure associating with the colorbar)

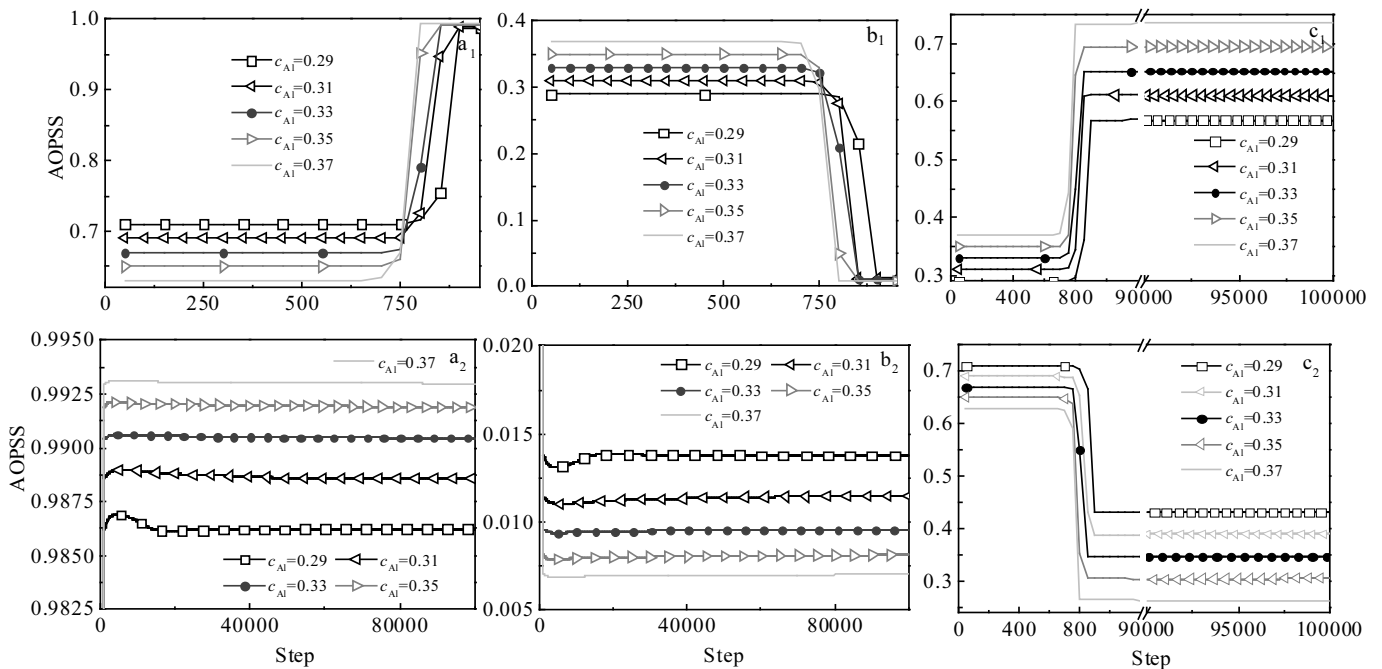


Fig.2 AOPSS curves of Fe_{Fe} (a_1, a_2), Al_{Fe} (b_1, b_2), Al_{Al} (c_1), and Fe_{Al} (c_2) in B2-FeAl phase at 853 K: (a_1, b_1) the AOPSS change in early stage; (a_2, b_2) the entire equilibrium state of AOPSS

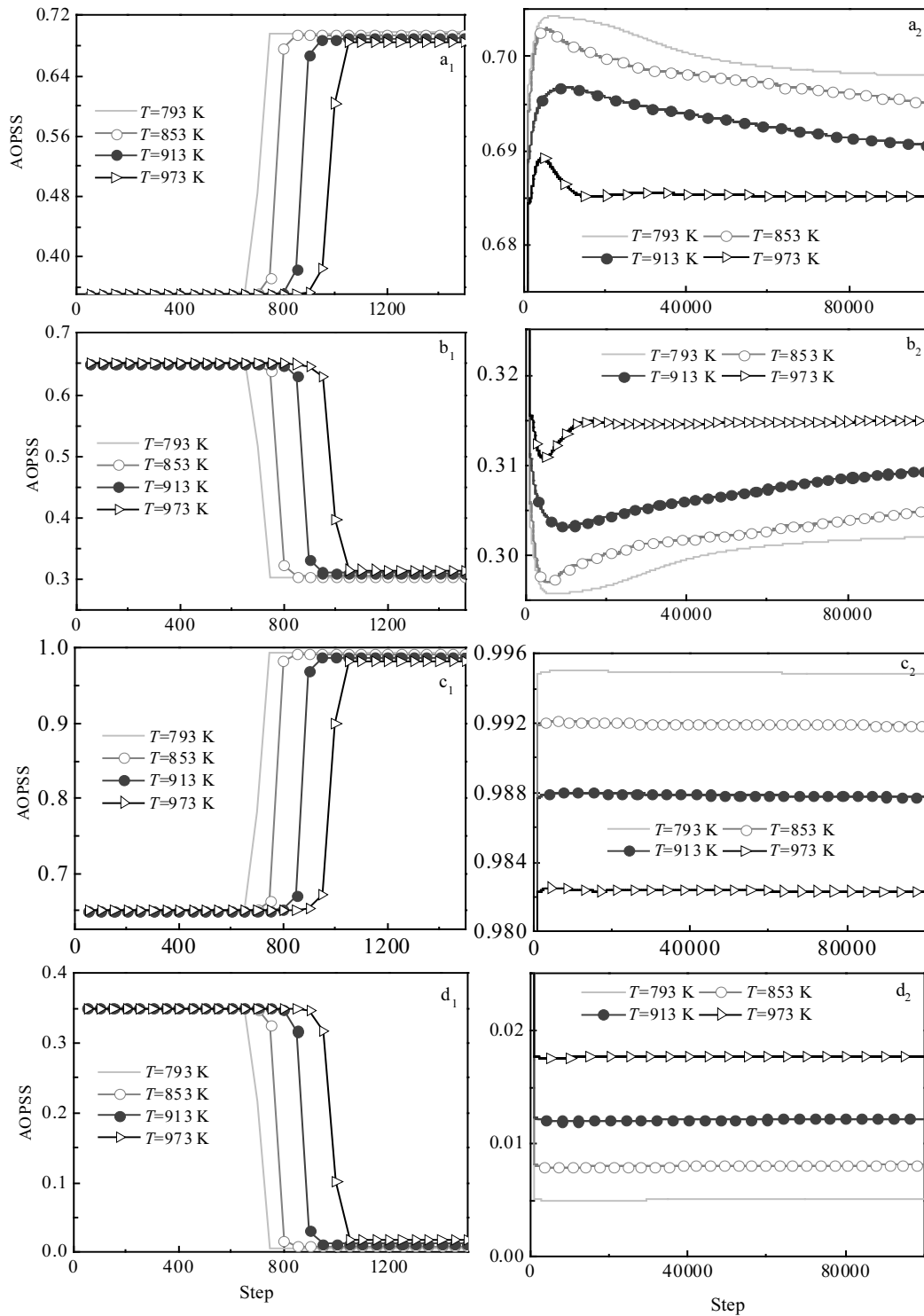


Fig.3 AOPSS curves of Al_{Al} (a₁, a₂), Fe_{Al} (b₁, b₂), Fe_{Fe} (c₁, c₂), Al_{Fe} (d₁, d₂) in B2-FeAl phase at different temperatures; the Al concentration is $c_{Al}=0.35$; (a₁, b₁, c₁, d₁) show the AOPSS change in early stage of ordering; (a₂, b₂, c₂, d₂) show the entire equilibrium state of AOPSS

solid solution condition, the system generates new atomic arrangements to minimize the total free energy. Consequently, the Fe and Al atoms are re-distributed from the initial disordered state, which means that the ordering

process enters into the SASP. As mentioned above, the alloy system quickly becomes ordered through the congruent ordering procedure, which is characterized by the sharp rise/drop in AOPSS curves of different sublattices. The

AOPSS variation means all atoms rearranging. In SASP, Fe site occupancy increases at r in time t . As there exists the relationship $\Phi_{\text{Al}}(r,t) + \Phi_{\text{Fe}}(r,t) = 1$, Al site occupancy correspondingly decreases in those lattices. Consequently, the Fe-sublattice forms on these sites. Conversely, those sites having an inverse AOPSS change construct the Al-sublattice. In Fig.2a₁, 2b₁, 2c₁ and 2c₂, it can be seen that the SASP is a short period compared with the whole aging process. By comparing the time at which the curves start to rise in Fig.2a₁, 2b₁ and 2c₁, it is evident that the SASP starts and ends earlier in a higher c_{Al} situation. In Fig.2a₂ and 2c₁, the AOPSS of Fe and Al in their own sites cannot reach to 1 at the end of equilibrium period, which means that there exist antisite defects. Fig.2b₁, 2b₂ and 2c₂ show two types of antisite defects, Al_{Fe} and Fe_{Al} , in the FeAl phase. Antisite defects are formed when the SASP ends. The flat curves (after $t=1000$) in Fig.2b₂ and 2c₂ demonstrate the existence of two antisite defects in the equilibrium period. As can be seen from Fig.2a₁ and 2a₂, when the Al concentration increases, the AOPSS of Fe increases. Because one lattice site can only accommodate one atom, the AOPSS of Al correspondingly decreases in Fe-sublattice (namely, Al_{Fe} antisite defects decrease). For the Al_{Fe} antisite defect (Fig.2b₁ and 2b₂), it decreases with the increase of Al concentration. Therefore, the increase of Al concentration benefits the long range order in Fe-sublattice. As for the Al-sublattice, there exists a positive relationship between site occupancy of Al and c_{Al} . Therefore, the formation of Fe_{Al} antisite defects is also hindered by increasing c_{Al} . Meanwhile, for different Al concentrations and different evolution times, the AOPSS value of Fe_{Al} is always much greater than the value of Al_{Fe} , which means that the main antisite defect type in B2-FeAl is Fe_{Al} . From above discussion, we can conclude that the increase of c_{Al} can enhance the site occupancies of Fe and Al, and impede the generation of Fe_{Al} and Al_{Fe} antisite defects. However, the change of c_{Al} does not alter the main type of antisite defect.

2.3 Effect of temperature on site occupancies and antisite defects

To reveal the effect of temperature on site occupancies of Al and Fe and the behavior of antisite defects, the aging processes of Fe-35%Al alloy at 793, 853, 913, 973 K were studied.

Curves of AOPSS change in FeAl ordered phase at different temperatures are shown in Fig.3. Fig.3a₁, 3b₁, 3c₁ and 3d₁ show the change of AOPSS in the early stage. The overlapped curves in Fig.3a₁, 3b₁, 3c₁ and 3d₁ demonstrate the incubation period during the decomposition process. Fe or Al has the same AOPSS in all lattice sites, and systems are disordered. As time progresses, the minimization of total free energy drives the ordering reaction proceeding to

the SASP. A large number of FeAl cell configurations are achieved through atoms ordering in a short time, which explains the Fe-, Al- AOPSS sharp variations (rise or decline) in different lattice sites. The gaps between steep curves (Fig.3a₁, 3b₁, 3c₁, 3d₁) reveal that temperature has obvious influence on AOPSS: the solute segregation is delayed by high temperature.

Curves in Fig.3a₂, 3b₂, 3c₂ and 3d₂ show the equilibrium period of ordering course. B2 structure forms as soon as system enters equilibrium period. Curves of AOPSS indicate that the spatial configuration of B2-FeAl lattice keeps stable from the beginning of equilibrium period. Curves in Fig.3a₂ and 3c₂ reveal that the increase of T hampers the abilities of Fe and Al locating in their own ideal sublattice sites. The effect of T on antisite defects is evident. From Fig.3b₂ and 3d₂, it is obvious that the increase of T facilitates the formation of antisite defects Fe_{Al} and Al_{Fe} . Meanwhile, the value of Fe_{Al} is always much greater than that of Al_{Fe} in equilibrium period, and the main antisite defect type is Fe_{Al} . Therefore, similar to Al concentration situations in Section 2.2, temperature cannot alter the main antisite defect type as well.

3 Conclusions

- 1) The ordering process undergoes three stages: incubation period, solute atoms segregation period and equilibrium period. The beginning of solute atoms segregation period and equilibrium are delayed by decreasing Al concentration or increasing the temperature.
- 2) The site occupancies and antisite defects have a close correlation with the temperature. As the temperature increases, site occupancies of Fe and Al gradually decrease in their own ideal sublattices, but the antisite behaviors of Fe and Al are increasingly promoted.
- 3) The rise of Al concentration can increase the site occupancy abilities of Al in Al-sublattice and Fe in Fe-sublattice. Meanwhile, the antisite behaviors of Fe and Al are re-strained.
- 4) Fe_{Al} is the main type of antisite defect in FeAl phase. It is not altered by temperature and Al concentration.

References

- 1 Zheng Y B, Wang F, Ai T T et al. *Journal of Alloys and Compounds*[J], 2017, 710: 581
- 2 Schaefer H E, Frenner K, Wuschum R. *Intermetallics*[J], 1999, 7(3-4): 277
- 3 Hanc A, Kansy J, Dercz G et al. *Journal of Alloys and Compounds*[J], 2009, 480: 84
- 4 Huang Y Y, Lu Y Q, Zhu Y Y et al. *Nuclear Instruments and Methods in Physics Research B*[J], 2009, 267: 3182
- 5 Cadel E, Fraczkiewicz A, Blavette D. *Materials Science and Engineering A*[J], 2001, 309-310: 32

- 6 Lindahl B B, Burton P B, Selleby M. *Computer Coupling of Phase Diagrams and Thermochemistry*[J], 2015, 51: 211
- 7 Gururajan M P, Abinandanan T A. *Materials Science and Engineering A*[J], 2002, 329-331: 388
- 8 Kupka M. *Journal of Alloys and Compounds*[J], 2007, 437: 373
- 9 Nogueira R N, Schon C G. *Intermetallics*[J], 2005, 13: 1233
- 10 Rio J D, Diego N D, Jimenez J A et al. *Intermetallics*[J], 2010, 18(7): 1306
- 11 Banerjee R, Amancherla S, Banerjee S et al. *Acta Materialia*[J], 2002, 50: 633
- 12 Khachaturyan A G. *Theory of Structural Transformation in Solids*[M]. New York: Wiley, 1983
- 13 Lu Y L, Zhang L C, Chen Y P et al. *Intermetallics*[J], 2013, 38: 144
- 14 Lu Y L, Lu G M, Liu F et al. *Journal of Alloys and Compounds*[J], 2015, 637: 149
- 15 Zhang J, Chen Z, Wang Y X et al. *Superlattices and Microstructures*[J], 2013, 64: 251
- 16 Hou H, Zhao Y H, Zhao Y H. *Materials Science and Engineering A*[J], 2009, 499: 204
- 17 Chen L Q. *Scripta Metallurgica et Materialia*[J], 1993, 29: 683
- 18 Chen L Q, Khachaturyan A G. *Scripta Metallurgica et Materialia*[J], 1991, 25: 61
- 19 Chen L Q, Khachaturyan A G. *Acta Metall Mater*[J], 1991, 39: 2533
- 20 Wang Y Z, Chen L Q, Khachaturyan A G. *Physical Review B*[J], 1992, 46: 11 194
- 21 Yasuda H Y, Nakano K, Nakajima T et al. *Acta Materialia*[J], 2003, 51: 5101
- 22 Zhao R D, Zhu J C, Liu Y et al. *Journal of Materials Science*[J], 2012, 47: 3376
- 23 Zhou Z C. *Materials Science and Engineering A*[J], 2006, 442: 82
- 24 Liu L L, Wu X Z, Wang R et al. *Computational Materials Science*[J], 2015, 103: 116
- 25 Sundman B, Ohnuma I, Dupin N et al. *Acta Materialia*[J], 2009, 57: 2896

B2-FeAl 有序相中成分与温度对占位与反位缺陷的影响: 相场法研究

王 锐¹, 王永欣¹, 胡 石², 陈 铮¹, 程岩峰¹

(1. 西北工业大学 凝固技术国家重点实验室, 陕西 西安 710072)

(2. 中国民用航空飞行学院, 四川 广汉 618307)

摘 要: 原子占位与反位缺陷对金属间化合物合金的物理与机械性能产生巨大的影响。B2-FeAl 作为一种具有优异性能的材料, 研究其中的原子占位与反位缺陷具有十分重要的意义。本研究利用相场方法研究了 B2-FeAl 有序相中铝浓度与温度对原子占位与反位缺陷变化趋势的影响。结果表明, 铝浓度的增加或者温度的降低能够加速母相中的溶质原子分离, 进而使得铝原子占位、铁原子占位以及反位铁或铝更早达到平衡态。特别地, 铝浓度的升高或温度的降低能够增强铝和铁的占位, 并减少 2 种类型的反位缺陷。此外, 研究结果还表明铝浓度或者温度的变化不能改变 B2-FeAl 有序相中主要的反位缺陷类型。

关键词: B2-FeAl; 占位; 反位缺陷; 温度与成分; 相场

作者简介: 王 锐, 男, 1986 年生, 博士生, 西北工业大学凝固技术国家重点实验室, 陕西 西安 710072, E-mail: wangkun11811@163.com